J Mater Sci (2008) 43:5300–5304
DOI 10.1007/s10853-008-2761-4

# Weldability in dissimilar welds between Type 310 austenitic stainless steel and Alloy 657

H. Naffakh · M. Shamanian · F. Ashrafizadeh

Received: 15 November 2007 / Accepted: 29 May 2008 / Published online: 24 June 2008


**Abstract** Microstructural evolution and solidification cracking susceptibility of dissimilar metal welds between Type 310 austenitic stainless steel and Inconel 657, a nickel-based alloy, were studied using a combination of electron microscopy analysis and Varestraint testing techniques. In addition, the effect of filler metal chemistry on the fusion zone composition, microstructure, and resultant weldability was investigated. The good cracking resistance of welds prepared with Inconel A was due to a small amount of secondary phase (NbC) and narrow solidification temperature range. The relatively poor cracking resistance of welds prepared with Inconel 82 and Type 310 stainless steel (310 SS) was a result of a wide solidification temperature range and an increase in the amount of secondary phases. Consequently, it is concluded that for the joint between Inconel 657 and 310 SS, filler material of Inconel A offers the best weldability.

## Introduction

50Ni–50Cr–Nb alloy, which was commercially introduced as Inconel 657, and Type 310 austenitic stainless steel are widely used in petrochemical and power generation industries [1, 2]. Inconel 657 contains Nb additions for improved hot corrosion resistance. However, in the case of alloy welding, during solidification of the weld metal, Nb segregates preferentially to the terminal liquid due to the low solubility of Nb in the austenite phase and therefore the first solidified liquid is depleted in Nb. In addition, the low diffusion rate of Nb in austenite phase does not allow Nb to diffuse to the dendrite cores. Therefore, elimination of the concentration gradient cannot be done. To compensate this effect, nickel-based filler metals such as Inconel 82, Inconel 182, Inconel 52, Inconel A, and Inconel 617 are often utilized during dissimilar fusion welding of these types of alloys [2–4]. The final distribution of Mo and Nb will be controlled by the filler metal composition, welding parameters (which control the dilution and resultant nominal weld metal composition) and the segregation potential of each element. In addition, interactive effects may exist in which the segregation potential of an alloying element depends on the nominal weld composition. These factors govern the solidification behavior and resultant hot cracking susceptibility of the fusion zone. Therefore, since wide ranges of weld metal composition are potentially possible in practice, a large variation in the fusion zone cracking susceptibility may happen. However, there is no detailed study in the literature investigating the relationship between nominal weld composition, fusion zone microstructure and resultant weldability for dissimilar metal weld joints between Inconel 657 and Type 310 stainless steel. Thus, the objective of this research was to characterize the microstructures and weldability of fusion welds in dissimilar welding between Inconel 657 and Type 310 austenitic stainless steel as a function of filler metal composition, using Inconel 82, Inconel A, Inconel 617, and 310 stainless steel.

## Materials and methods

The base materials used in the study were 12 mm thick plates of Type 310 stainless steel and Inconel 657. The former was in the solution-annealed condition and the latter was in the as-cast condition. The four consumables examined were

H. Naffakh (✉) · M. Shamanian · F. Ashrafizadeh
Department of Materials Engineering, Isfahan University of Technology, Isfahan 84156-83111, Iran
e-mail: homam-naffakh@ma.iut.ac.ir

**Table 1** Nominal composition of the base and filler materials (wt.%)

| Elements | Base metals | | Filler materials | | | |
|---|---|---|---|---|---|---|
| | 310 SS | Inconel 657 | Inconel 82 | Inconel 617 | Inconel A | 310 SS |
| C | Max 0.1 | Max 0.2 | Max 0.1 | Max 0.1 | Max 0.1 | Max 0.1 |
| Si | 1 | 1 | 0.5 | 1 | 1 | 1 |
| Mn | 2 | 1 | 3 | 2 | 3 | 2 |
| Fe | Rem. | 1 | 3 | 5.5 | 12 | Rem. |
| Cr | 26 | 45 | 20 | 25 | 15 | 26 |
| Mo | – | – | – | 10 | 1.5 | – |
| Co | – | – | – | 10 | – | – |
| Ti | – | – | 1 | 0.6 | – | – |
| Nb | – | 1 | 3 | 1 | 2.5 | – |
| Al | – | – | – | 1 | – | – |
| Ni | 21 | Rem. | Rem. | Rem. | Rem. | 21 |
| Cu | – | – | 0.5 | 0.5 | 0.5 | 0.75 |

Inconel 82, Inconel A, Inconel 617, and Type 310 stainless steel. The nominal compositions of the base materials and the undiluted filler materials are given in Table 1.

Hot cracking was studied by performing the longitudinal Varestraint test to compare filler materials. Prior to Varestraint testing, welded joints between the base materials were made, using each of the four filler materials, employing a V groove edge preparation with an included angle of 75°, prepared root gap opening of 2.5 mm, and a root face of 1 mm. Laboratory scale specimens with dimensions of $150 \times 25 \times 3.2$ mm$^3$ were then prepared for Varestraint testing. Subsequently, hot cracking susceptibility of the various weld metals was tested on a moving torch Varestraint hot cracking test device. The augmented bending strain $e$ applied to the surface of the test specimen is related to the radius of the die block by the equation $e = t/2R$, where $t$ is the specimen thickness and $R$ is the radius of the die block [5, 6]. The strain levels applied were 1, 2, and 4%. The welding parameters used during Varestraint testing were kept constant as follows: current = 130 A, voltage = 18 V and travel speed = 4.5 mm/s. Afterwards, both total crack length (TCL) and maximum crack length (MCL) were used as the criteria for evaluating the hot cracking susceptibility of the weld metals. Transverse sections of the welds were metallographically characterized after etching in Marble's solution (10 g $CuSO_4$ + 50 mL HCl + 50 mL $H_2O$). The weldments were evaluated using light optical microscopy (LOM) and scanning electron microscopy (SEM).

## Results and discussions

### Microstructures

The fusion zone microstructure of Inconel 82 weld metal is shown in the backscattered electron image in Fig. 1a. The microstructure is fully austenitic, as expected. Furthermore, it is seen that NbC precipitates (brightly imaging precipitates) have formed in the interdendritic regions (Fig. 1b). There is no evidence of the formation of lamellar $\gamma$/laves eutectic in the interdendritic regions. The NbC precipitates can lead to an increase in solidification cracking tendency.

The backscattered electron image in Fig. 1c shows the fusion zone of Inconel A weld metal. Inconel A weld metal is similar to Inconel 82 in that it has a considerable amount of niobium (2.5%), but its iron content (12%) is much greater than Inconel 82 weld metal (3%). The presence of iron in nickel-based superalloys leads to a decrease in niobium solubility in austenite phase. In an iron-containing nickel–chromium solid solution, the ability of Nb to remain in solution is limited [2]. Under these conditions, partitioning of Nb to the interdendritic regions in the weld metal is increased. Segregation of alloying elements can lead to expansion of the brittle temperature range (BTR) and an increase in constitutional supercooling. However, no low-melting phases were observed in the interdendritic and intergranular regions (Fig. 1d).

Fig. 1e shows the fusion zone microstructure of the Inconel 617 filler material. The Mo partition coefficient decreases as the iron content of the weld increases (i.e., as the dilution level increases). Moreover, this figure illustrates the fully dendritic microstructure of Inconel 617 weld metal which consists of columnar dendrites. These dendrites are a result of strong Mo partitioning to the terminal interdendritic liquid. This structure is coarse, and it is well-known that a coarse dendritic structure is more prone to hot cracking than fine structures [7–9]. Figure 1f is a backscattered electron image showing the microstructure of the Type 310 SS fusion zone. Since the weld metal contains a small amount of copper, the formation of secondary phases at grain boundaries makes the weld metal susceptible to hot cracking.

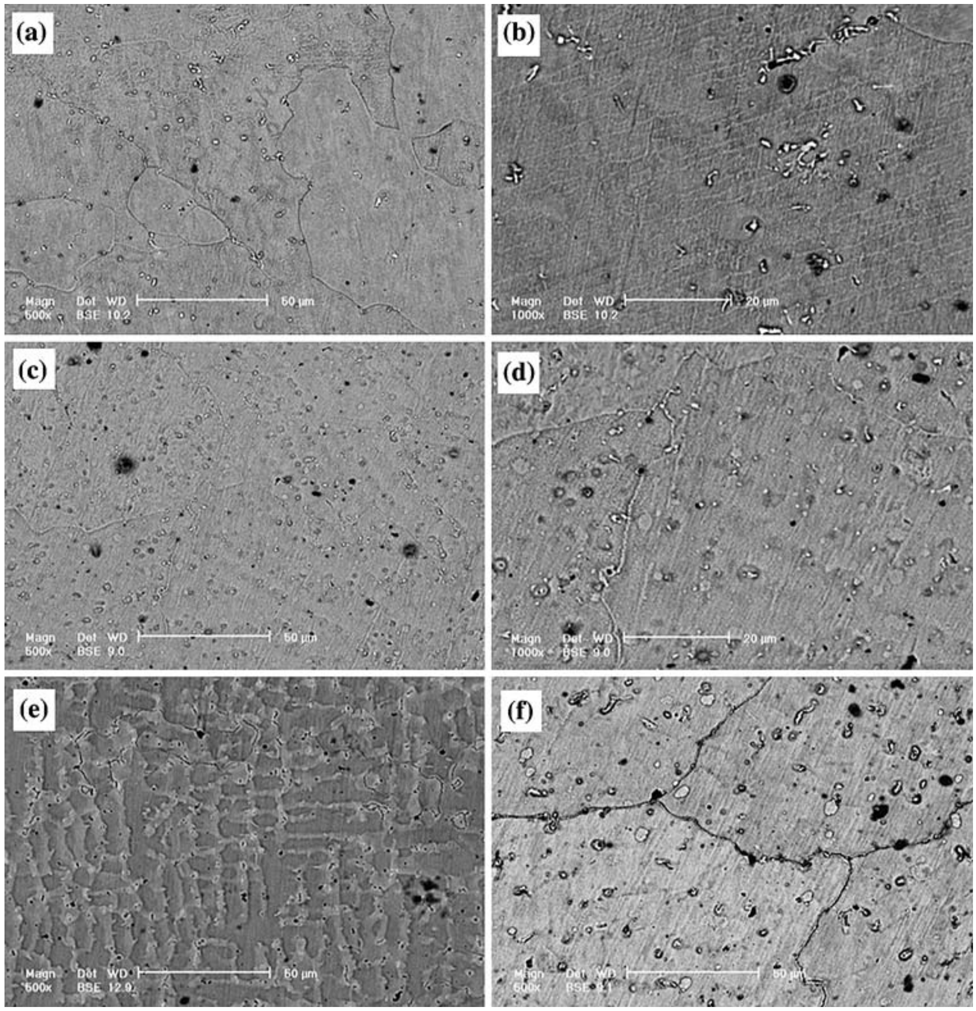


**Fig. 1** Backscattered electron images of the welds: (**a**) Inconel 82, (**b**) Inconel 82 at higher magnification (the brightly imaging features are Nb-enriched precipitates), (**c**) Inconel A, (**d**) Inconel A at higher magnification, (**e**) Inconel 617, and (**f**) 310 SS

## Hot cracking susceptibility

The results of the longitudinal Varestraint testing are given in Fig. 2, which shows the dependence of total crack length and maximum crack length on the applied strain. It is clear from the plots that Inconel A weld metal shows the least susceptibility to hot cracking. The presence of iron in Inconel A solid solution decreases niobium solubility in austenite, but higher amounts of nickel and lower amounts of chromium in this weld metal can dissolve an increased amount of niobium in austenite and reduce segregation of Nb along the boundaries as well. The occasional anomalous behavior, observed in some cases, might be attributed to the nature of produced samples used for testing. In the conventional Varestraint testing, wrought base metal specimens are used. However, in this investigation, weld metals were first produced using the respective filler materials and were then remelted during the Varestraint testing. Minor variations in dilution at the region of strain application might be responsible for the observed behavior.

In Fig. 2a it can be noticed that none of the four weld metals, except Inconel 82, exhibited cracking at 1% strain signifying the threshold strain. The total crack length in Inconel 82 and Inconel 617 does not increase as the strain is increased from 2% to 4%, indicating a saturation effect at 2% strain. It may also be observed in Fig. 2b that the maximum crack length in the Inconel A weld metal is the lowest among the investigated weld metals. According to the above-mentioned results, Inconel 82 shows a higher tendency for solidification cracking than other filler materials. The obtained result is in agreement with previous investigations [10].

Additionally, Type 310 SS weld metal demonstrates a weak resistance to hot cracking. The formation of a network of low-melting phases in the fusion zone might be the most effective factor in the hot cracking sensitivity in 310 SS weld metal. None of the welds shows crater cracking except the Type 310 SS weld metal that displays crater cracks in all the applied stresses.

The microstructures of the cracked regions are shown in Fig. 3a–f. The cracking appeared to be mostly intergranular;

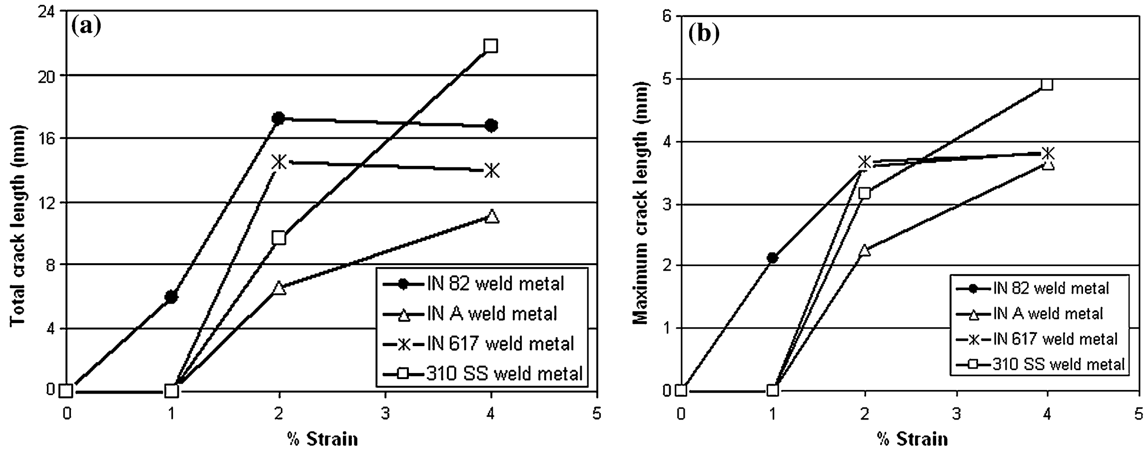


**Fig. 2** Varestraint testing results: (**a**) total crack length in fusion zones, (**b**) maximum crack length in fusion zones

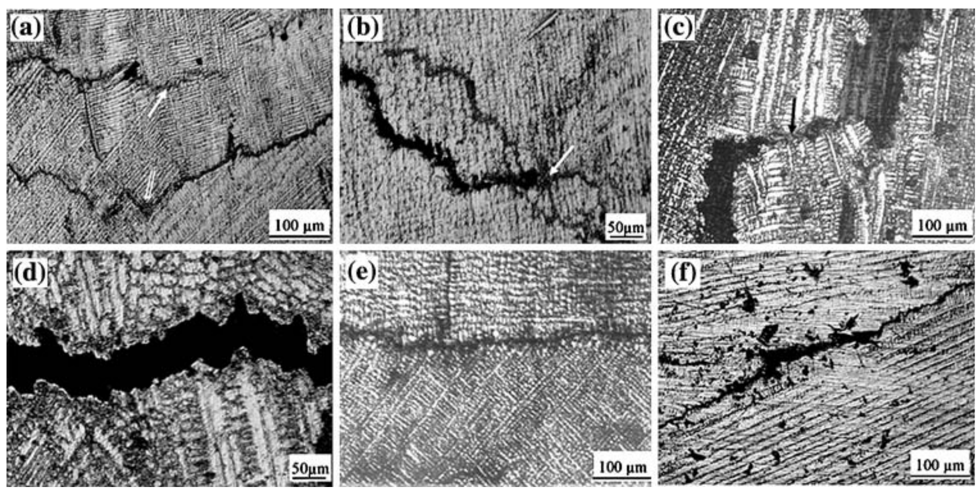


**Fig. 3** (**a**) Solidification cracking (arrow) in Inconel 82 weld metal, (**b**) Solidification cracking (arrow) in Inconel 82 weld metal, (**c**) solidification cracking (arrow) in Inconel 617 weld metal, (**d**) solidification cracking in Inconel 617 weld metal at higher magnification, (**e**) solidification cracking in Inconel A weld metal, and (**f**) solidification cracking in 310 SS weld metal

some cracks along the substructure boundaries can also be observed. The extensive cracking in all weld metals might be a result of the predominantly austenitic mode of solidification and pronounced dendritic morphology.

It is concluded that in the case of Inconel 82 and Inconel A weld metals the presence of niobium governs the formation of low-melting phases in the interdendritic and intergranular regions. On the other hand, in Inconel 617 weld metal, susceptible phases to solidification cracking can form due to the presence of copper, aluminum, and titanium. The probable presence of Cu in the low-melting phases can decrease the resistance of 310 SS weld metal to hot cracking.

## Conclusions

All the weld metals investigated herein had fully austenitic microstructures. The $\gamma$/NbC eutectic structure was formed in interdendritic regions of Inconel 82 weld metal. However, no low-melting phases were observed by SEM in the interdendritic and intergranular regions of Inconel A weld metal. Inconel 617 weld metal displayed a more distinctive columnar dendritic structure, in comparison to Inconel 82 and Inconel A weld metals. There was a continuous network of low-melting phases in the grain boundaries of Type 310 SS weld metal. Based on the Varestraint results, Inconel A weld metal showed the least susceptibility to hot cracking whereas Inconel 82 showed the highest tendency to solidification cracking. Type 310 SS filler metal also exhibited weak resistance to hot cracking. It can be concluded that of the materials evaluated, Inconel A filler material provides the best weldability for joints between Type 310 stainless steel and Inconel 657.

## References

1. Belloni G, Caironi G, Gariboldi A (2001) Lo Conte Politecnico di Milano A Transactions SMiRT16 Paper 1546
2. Dupont JN, Banovic SW, Marder AR (2003) Weld J 82:125

3. Lee HT, Jeng SL, Yen CH, Kuo TY (2004) J Nucl Mater 335:59. doi:10.1016/j.jnucmat.2004.06.004
4. Rowe MD, Crook P, Hoback GL (2003) Weld J 82:313
5. Savage WF, Lundin CD (1966) Weld J 45:497
6. Savage WF, Lundin CD (1965) Weld J 44:433
7. Wang N, Mokadem S, Rappaz M, Kurz W (2004) Acta Mater 52:3173. doi:10.1016/j.actamat.2004.03.047
8. Kuo T-Y, Lee H-T (2002) Mater Sci Eng A 338:202
9. Sireesha M, Shankar V, Albert SK, Sundaresan S (2000) Mater Sci Eng A 292:74. doi:10.1016/S0921-5093(00)00969-2
10. Sireesha M, Albert SK, Shankar V, Sundaresan S (2000) J Nucl Mater 279:65. doi:10.1016/S0022-3115(99)00275-5